Vietnam Journal of Earth Sciences, 48(4), 513−534, https://doi.org/10.15625/2615-9783/24668

Vietnam Journal of Earth Sciences
https://vjs.ac.vn/index.php/jse

Urban development management in Dien Bien Phu City: An integrated approach using multi-source remote sensing, machine learning, and planning maps

Bui Thi Ngoc Lan[1], Nguyen Manh Hung[2,3*], Vu Anh Tuan[2], Dao Duy Toan[4], Asami Hideki[5], Nguyen Cong Giang[2,6]

[1]*Faculty of Urban Management - Hanoi Architectural University*
[2]*Vienam National Space Center, Vietnam Academy of Science and Technology, Hanoi, Vietnam*
[3]*Graduate University of Science and Technology, VAST, Hanoi, Vietnam*
[4]*Faculty of Bridge and Road, Hanoi University of Civil Engineering, Hanoi, Vietnam*
[5]*Former President of Nikken Sekkei Civil Engineering*
[6]*Faculty of Architecture and Engineering, University of Phuong Dong*

Received 13 January 2026; Received in revised form 20 February 2026; Accepted 19 May 2026

ABSTRACT

Sustainable urban development management in mountainous cities with complex basin topography is becoming a formidable challenge for urban planners amidst rapid urbanization. This study quantifies the land use/land cover (LULC) dynamics in Dien Bien Phu City from 2018 to 2025 using an integrated framework that combines multi-temporal Sentinel-2 imagery, Shuttle Radar Topography Mission Digital Elevation Model (SRTM DEM), and the Random Forest machine learning algorithm on the Google Earth Engine platform. The classification results achieved high reliability, with overall accuracy (OA) ranging from 94.2% to 98.8% and Kappa coefficients (Kappa) exceeding 0.96. Spatial analysis reveals a pronounced structural shift in land cover: built-up areas increased significantly from 8.8% in 2018 to 12.4% in 2025, while forest cover declined sharply from 35.1% to 26.7%. Notably, bare land accounted for a substantial proportion (14.1%) by 2025, potentially indicating land preparation activities and reflecting possible short-term fluctuations in plantation forest cover. The results further suggest that urban growth is transitioning from a historically monocentric pattern towards a more polycentric model, primarily expanding into southern and western corridors. By benchmarking these findings against the 2045 General Planning Vision, this study identifies potential conflict zones between urban expansion and ecological conservation in mountainous buffer areas. These findings provide a scientific basis for urban authorities to regulate land-use conversion, particularly in high-risk basin foothill zones, while simultaneously addressing the imbalance between infrastructure expansion and ecological preservation. In particular, the spatial delineation of urbanization pressures provides actionable guidance for establishing greenbelts and optimizing urban growth boundaries in accordance with the 2045 General Planning Vision, thereby enhancing the long-term climate resilience of basin-type cities under accelerating environmental change.

Keywords: Sustainable urbanization, Urban planning, Remote sensing, Machine learning, Basin-type cities.

1. Introduction

Urbanization has become one of the most dominant global processes shaping socio-economic development in the 21st century. According to the United Nations, more than 55% of the world's population currently

*Corresponding author, Email: nmhung@vnsc.org.vn

resides in urban areas, and this proportion is projected to reach nearly 70% by 2050, with the fastest growth occurring in developing countries (United Nations, 2022). While urbanization plays a critical role in economic growth and social transformation, rapid and often unplanned urban expansion has led to profound environmental challenges, including LULC change, ecological degradation, loss of urban green spaces, and the intensification of the urban heat island (UHI) effect (Seto et al., 2012). In Vietnam, recent studies have highlighted the significance of deep learning technologies in monitoring land cover dynamics. For instance, Nguyen Thanh et al. (2025) used deep neural networks (DNNs) integrated with high-resolution UAV imagery to map forest cover changes, confirming that anthropogenic activities are the primary drivers of land cover transformation in mountainous regions. These impacts are particularly pronounced in cities experiencing accelerated infrastructure-led development, where the conversion of natural surfaces into impervious built-up areas disrupts local climate regulation and ecosystem services (Manoli et al., 2019). Furthermore, a classification framework was proposed that integrates EfficientNet with hyperparameter optimization algorithms, achieving high accuracy across diverse Vietnamese landscapes from lowlands to mountainous regions, thereby providing a powerful tool for nationwide urban monitoring and resource management.

In recent decades, remote sensing technologies have emerged as indispensable tools for monitoring urban dynamics at multiple spatial and temporal scales. Satellite missions such as Landsat and Sentinel are freely available and provide consistent, long-term observations that enable detailed analysis of LULC changes, urban expansion patterns, and surface biophysical characteristics (Wulder et al., 2022). Concurrently, advances in machine learning (ML) techniques have significantly improved the accuracy and robustness of urban land cover classification. Algorithms such as Random Forest (RF), Support Vector Machines (SVM), and, more recently, deep learning models (e.g., Convolutional Neural Networks - CNNs) have been widely adopted owing to their ability to handle high-dimensional data, nonlinear relationships, and complex spectral features inherent in urban environments (Tamiminia et al., 2020). The integration of remote sensing and ML has therefore become a well-established and powerful framework for urban studies (Ma et al., 2019; Weng, 2012). This approach effectively supports a wide range of applications, from modeling urban growth trajectories to assessing environmental impacts such as the surface urban heat island effect (Azizi et al., 2022; Weng, 2001), thereby providing critical empirical evidence for sustainable spatial planning (Herold et al., 2003). Over the past few years, the application of machine learning algorithms in earth sciences has seen significant growth in Vietnam, ranging from forest cover monitoring (Nguyen Thanh et al., 2025), natural hazard detection in mountainous areas (Ngo Van et al., 2025), to environmental parameter prediction (Nguyen et al., 2025). Among various models, Random Forest remains a highly reliable method for spatial classification and characterization in diverse Vietnamese landscapes (Nguyen Trinh Duc et al., 2025). Building on these advancements, this study focuses on leveraging these robust techniques to address the specific challenges of urban monitoring in complex terrains.

Despite these advances, several critical research gaps remain. First, the majority of existing studies focus on megacities and large metropolitan areas located in lowland or coastal regions, where terrain is relatively homogeneous and urban expansion follows more predictable spatial patterns. In contrast, mountainous and basin-shaped cities, which are common in many developing countries, have received far less attention (Zhou et al.,

2019). These cities are characterized by complex topography, strong elevation gradients, and a high degree of spatial intermixing between built-up areas, forests, agricultural land, and bare soil, resulting in highly heterogeneous spectral responses. Second, many previous studies rely primarily on satellite-derived features and often fail to adequately address quality assurance and quality control through cross-validation with high-resolution imagery or ground-based data, particularly in topographically fragmented regions. This limitation can lead to uncertainty in classification results and reduce the reliability of derived urban management indicators.

Dien Bien Phu City, located in Northwestern Vietnam, represents a particularly relevant yet underexplored case. As a historically significant city and the economic and administrative center of the Northwest region, Dien Bien Phu is undergoing rapid urban transformation driven by major infrastructure investments, including airport expansion and transport network development (Ministry of Construction & People's Committee of Dien Bien Province, 2024). Urban growth in the city is increasingly encroaching on surrounding mountainous areas and forested slopes, intensifying the trade-off between economic development, environmental protection, and disaster risk management (Dien Bien Province Department of Natural Resources and Environment, 2024). The basin-shaped topography further amplifies local microclimatic changes, increasing the susceptibility to heat accumulation, landslides, and ecological imbalance as impervious surfaces expand toward mountain foothills.

There is a need for reliable, scalable, and spatially explicit approaches to support urban development management in Dien Bien Phu and similar mountainous cities. This study addresses the identified research gaps by leveraging multi-source remote sensing data and machine learning techniques to analyze urban expansion dynamics and provide scientifically grounded insights for sustainable urban management. By focusing on a medium-sized mountainous city rather than a megacity, this research broadens the geographical and methodological scope of urban remote sensing studies and offers practical implications for urban planning and climate-resilient development in complex terrain.

2. Materials and Methods

2.1. Study area

Dien Bien Phu City (the pre-merger period) serves as the administrative, political, economic, and cultural hub of Dien Bien Province. The city is located in Northwestern Vietnam and shares a strategic border with Laos via the Tay Trang International Border Gate (Fig. 1). It is situated within a topographically constrained yet strategically located basin system. The landscape is defined by the Muong Thanh Valley, encircled by steep mountain ranges with elevations ranging from 473 m to 1,048 m above sea level (asl). This complex basin topography creates a "confined" urban space, with the urban core concentrated at lower elevations (477 m to 483 m), making it highly susceptible to increased impervious surfaces (Ministry of Construction & People's Committee of Dien Bien Province, 2024). The interplay between rapid urban expansion and this fragmented terrain poses significant ecological risks. As urban boundaries encroach upon the mountain foothills and slopes, the disruption of natural vegetation cover increases vulnerability to hazards, including landslides, debris flows, and sedimentation of the Nam Rom River system. Furthermore, the basin geometry amplifies local microclimatic challenges, such as heat accumulation and altered drainage patterns (Nguyen Thi Phuong et al., 2022).

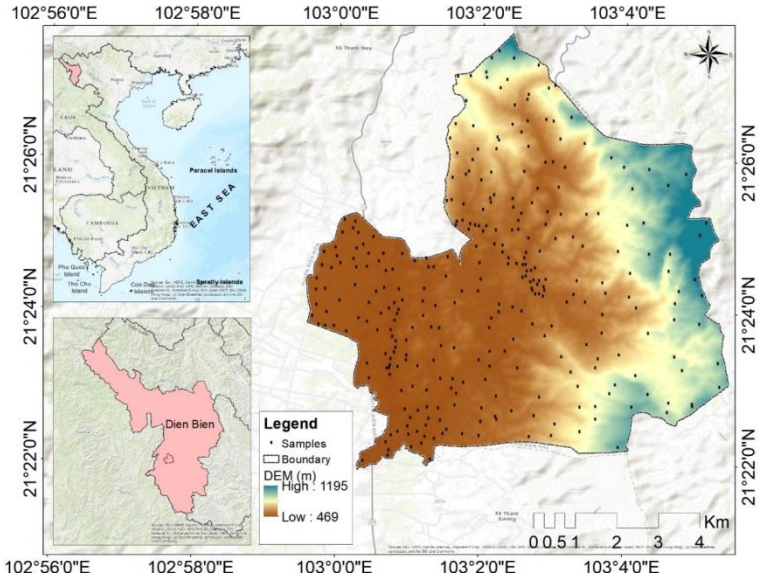

Figure 1. Study area

The city is undergoing a rapid transition from agro-forestry to a service-oriented economy, driven by trade, tourism, and infrastructure development (Dien Bien Provincial Statistics Department, 2024). Key initiatives, such as the Northern Mountains Urban Program, have acted as a primary catalyst for land-use conversion and infrastructure expansion (World Bank, 2014). However, while these developments drive economic momentum, the fragmented mountainous topography significantly increases construction costs and constrains urban spatial expansion, necessitating a balanced strategy between modernization and environmental stability. Consequently, the integration of remote sensing technologies for monitoring, analyzing, and supporting urban planning is imperative to enhance the efficiency of comprehensive and sustainable spatial management.

2.2. Data sources

This research utilizes a multi-source dataset to address the inherent challenges of land-cover classification in complex mountainous terrains such as Dien Bien Phu City (Belcore et al., 2020). The primary optical data source consists of Sentinel-2 (Level-2A) multi-temporal imagery with a 10 m spatial resolution, acquired from 2018 to 2025 via the Google Earth Engine (GEE) platform (Drusch et al., 2012). Selecting the dry season (January and February) in Northwestern Vietnam optimizes observation conditions by ensuring that cloud cover remains below 5% while maintaining vegetation's stable spectral characteristics. This facilitates clear differentiation between evergreen forests, agricultural land, and pre-construction infrastructure sites. Given the basin topography characterized by significant altitudinal variations, the SRTM DEM at 30 m resolution from the USGS was integrated as a critical input variable (Delalay et al., 2019). The inclusion of SRTM data not only mitigates errors induced by topographic shadowing but also helps accurately delineate vegetation types across different elevation belts and steep slopes, thereby substantially enhancing the precision of the final land-cover maps (Yin et al., 2022).

To facilitate cross-validation and error assessment, the study uses high-resolution

PlanetScope imagery (3 m) and historical Google Earth data for the corresponding periods. These ultra-high-resolution sources enable the detailed interpretation of fragmented objects within valleys and peri-mountainous residential areas (Houborg & McCabe, 2016). Consequently, they provide an independent source of training and validation samples, ensuring high reliability for land-cover change analysis within the highly dissected terrain of the study area (Acharki, 2022).

Table 1. The table describes detailed information about the data used

No	Sensor	Date of acquisition	Spatial resolution (m)	Data sources
1	Sentinel-2	14/02/2025	10 m	ESA
2		05/02/2024		
3		26/01/2023		
4		26/01/2022		
5		25/02/2021		
6		17/01/2020		
7		21/02/2019		
8		11/02/2018		
9	SRTM	2000	30 m	USGS
10	PlanetScope	28/04/2020 01/03/2025	3 m	Planet Labs
11	Google Earth	February 2020, April 2025		

Additionally, the Master Plan for Dien Bien Phu City to 2045, provided by the Dien Bien Department of Construction, was utilized as a spatial reference for the analysis.

2.3. Methods

This study establishes an integrated analytical framework leveraging multi-source remote sensing data and machine learning algorithms to quantify LULC dynamics for sustainable urban management. The general workflow (Fig. 2) initiates with the acquisition of Sentinel-2 (Level-2A) multi-temporal imagery as surface reflectance (SR) products via the GEE cloud platform. Rigorous cloud-masking and atmospheric correction procedures were implemented to ensure spectral consistency across bands. Since Sentinel-2 bands possess varying spatial resolutions (10 m, 20 m, and 60 m), all 20 m bands, specifically B11 and B12, required for NDBI calculation were resampled to a 10m resolution using the bilinear interpolation method. This preprocessing step ensures spatial consistency across all spectral indices and maintains the greatest possible detail for mapping urban features in the fragmented terrain of Dien Bien Phu City. To optimize the separability of complex surface features, a multidimensional feature set was constructed, incorporating original spectral bands, specialized indices such as NDVI, NDWI, and NDBI, and Digital Elevation Models (DEM) to mitigate topographic effects. Given the unique basin topography of Dien Bien Phu City, this study established a LULC classification schema comprising five core classes: Built-up (BU), Water (W), Forest (F), Agriculture (A), and Bare soil (BS). The training sample collection involved manual visual interpretation of high-resolution PlanetScope imagery (3 m) and cross-referencing with temporally matched data from Google Earth Pro. To enhance input data reliability, sample polygons were delineated within highly homogeneous areas and quantitatively validated through specific spectral indices: NDBI for urban and industrial zones, NDWI for the Nam Rom River system and local reservoirs, and NDVI for dense forest canopies. Agricultural samples were verified using multi-temporal analysis to accurately capture seasonal crop cycles, while bare soil points were extracted from active infrastructure sites or cleared land. The entire sample database was digitized in ArcGIS before being integrated into the GEE platform for classification.

The model training phase used the RF algorithm, a non-parametric classification approach that robustly handles multivariate data. A set of data samples was accurately labeled using the aforementioned

co-registered high-resolution PlanetScope and Google Earth imagery, and the data were then divided into training and validation sets (70% and 30%, respectively). The reliability of the LULC map series from 2018 to 2025 was validated using a confusion matrix, OA, and Kappa. Detailed statistics on sample size and spatial distribution are provided in Table 2 and Fig. 1. This framework provides a reliable baseline dataset for analyzing urban expansion trends in alignment with Dien Bien Phu City's spatial planning vision toward 2045.

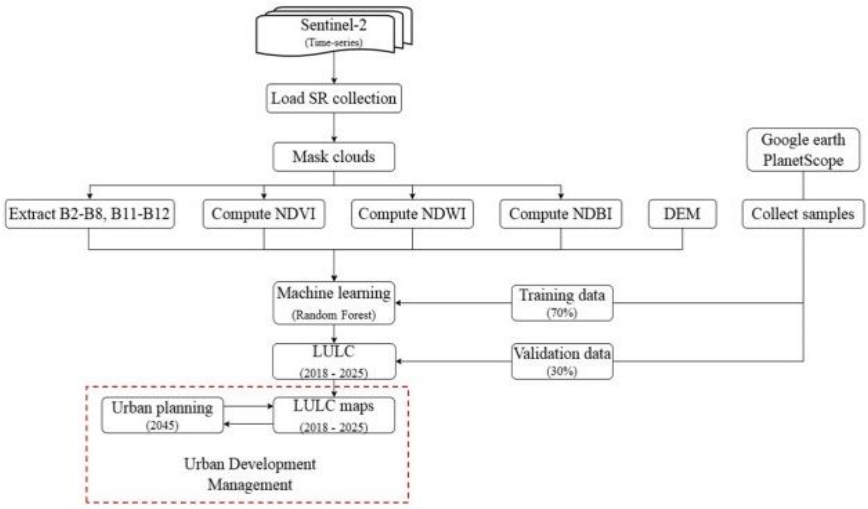

Figure 2. Workflow of the study

Table 2. Characteristics and number of training samples across years

LULC	Number of sample points/polygons								Description
	2018	2019	2020	2021	2022	2023	2024	2025	
BU	70/5	70/4	70/5	70/6	70/5	70/10	70/6	70/4	Residential areas, industrial zones, roads, and other impervious surfaces (concrete, asphalt).
F	70/5	70/4	70/8	70/8	70/7	70/6	70/6	70/4	Areas dominated by natural or plantation trees with high canopy cover, including evergreen and deciduous forests.
W	70/4	70/4	70/4	70/4	70/4	70/4	70/4	70/4	Rivers (Nam Rom river), reservoirs, ponds, and other open water surfaces.
A	70/6	70/4	70/5	70/5	70/6	70/5	70/5	70/4	Paddy fields, croplands, and perennial fruit trees.
BS	70/7	70/3	70/7	70/5	70/4	70/8	70/4	70/3	Exposed soil, construction sites (cleared land), and sparsely vegetated rocky areas.
Total samples	**982**	**800**	**1096**	**1051**	**1243**	**1433**	**1061**	**1064**	

2.3.1. Normalized Difference Vegetation Index (NDVI)

The Normalized Difference Vegetation Index (NDVI) is one of the most widely used spectral proxies for quantifying vegetation density and photosynthetic vigor. This index operates on the principle that healthy vegetation exhibits strong absorption in the red (Red) spectrum for photosynthesis while demonstrating high reflectance in the near-infrared (NIR) region due to the internal cellular structure of leaves (Rouse et al., 1974). The NDVI formula is presented in Equation (1). Utilizing Sentinel-2 imagery, NDVI is computed using Band 8 (NIR, 842 nm) and Band 4 (Red, 665 nm) at a 10 m spatial resolution:

$$NDVI = \frac{B_{NIR}+B_{Red}}{B_{NIR}-B_{Red}} \quad (1)$$

The application of NDVI facilitates a distinct differentiation between forest cover on mountainous slopes and peri-urban bare land areas in Dien Bien Phu.

2.3.2. Normalized Difference Water Index (NDWI)

To identify water bodies, such as the Nam Rom River system and local reservoirs, the Normalized Difference Water Index (NDWI) was employed. This index utilizes the green and near-infrared (NIR) bands to enhance moisture and open water surfaces while effectively suppressing background signals from vegetation and soil (McFeeters, 1996). The NDWI formula is presented in Equation (2). The calculation for Sentinel-2 imagery specifically incorporates Band 3 (560 nm) and Band 8 (842 nm):

$$NDWI = \frac{B_{Green} - B_{NIR}}{B_{Green} + B_{NIR}} \quad (2)$$

In basin-like environments, NDWI plays a pivotal role in mitigating noise from mountainous shadows in the Western ranges, which often exhibit spectral reflectance values similar to those of water bodies (Xu, 2006).

2.3.3. Normalized Difference Built-up Index (NDBI)

The Normalized Difference Built-up Index (NDBI) was employed to delineate impervious surfaces and urban infrastructure. This index leverages the high reflectance of construction materials (such as concrete and corrugated metal) in the short-wave infrared (SWIR) band compared to the near-infrared (NIR) band (Zha et al., 2003). The NDBI formula is presented in Equation (3). For Sentinel-2 imagery, the Band 11 (1610 nm) and Band 8 (842 nm) are integrated as follows:

$$NDBI = \frac{B_{SWIR} - B_{NIR}}{B_{SWIR} + B_{NIR}} \quad (3)$$

However, due to the spectral similarities between built-up areas and bare soil under arid conditions, this study incorporates additional topographic features to refine the NDBI classification results. This approach improves mapping accuracy for rapidly expanding infrastructure zones in the city center (X.-L. Chen et al., 2006).

2.3.4. Random Forest Algorithm

The RF algorithm was selected as the core classification framework for this study due to its robust performance on high-dimensional, nonlinear datasets (Hung et al., 2025).

As an ensemble learning technique, RF constructs a multitude of independent decision trees $\{h(x, \theta_k), k = 1, \dots\}$ where x is the input feature vector and θ_k are independent identically distributed random vectors (Breiman, 2001). The algorithm operates through the bootstrap aggregating (bagging) mechanism, where each tree is trained on a random subset of the training data $S_{bootstrap}$ sampled with replacement. During the construction of each tree, at each split node, only a random subset of m features (where m < M, and M is the total number of features) is selected to determine the optimal split based on the Gini Impurity index:

$$Gini(D) = 1 - \sum_{i=1}^{C} P_i^2 \quad (4)$$

where P_i is the relative frequency of class i in the dataset D, and C is the total number of land cover classes. The node split is chosen to maximize the information gain, thereby reducing the impurity in the resulting child nodes.

The final classification outcome is determined via a majority voting mechanism, which can be mathematically expressed as:

$$\hat{C} = mode\{h_1(x), h_2(x), \dots h_k(x)\} \quad (5)$$

where $\hat{C}$ is the predicted class for a given pixel x. This ensemble approach effectively reduces the correlation among individual trees, mitigates overfitting, and enhances resilience to spectral noise inherent in multi-temporal remote sensing data (Belgiu & Drăguţ, 2016).

Furthermore, the algorithm calculates Out-of-Bag (OOB) error for internal cross-validation, ensuring stable classification results across different time steps.

To optimize classification performance within the complex Dien Bien basin, the RF model was configured to integrate a high-dimensional feature space. This included spectral features from Sentinel-2 bands B2 through B8 and B11, B12, alongside key remote sensing indices (NDVI, NDWI, NDBI) to enhance the separability of spectrally similar classes. In addition to spectral data, the Digital Elevation Model (DEM) and its derived topographic variables were incorporated as critical auxiliary features. This integration allowed the RF model to exploit the vertical distribution of land-cover types, enabling accurate discrimination between built-up areas in the valley and barren soil on steeper slopes, a task that remains challenging with optical data alone in dissected mountainous topographies.

2.3.5. Accuracy Assessment

The accuracy of the LULC maps was systematically quantified using an independent validation dataset, prioritizing metrics that reflect the quality of individual classes rather than relying solely on traditional indices. Specifically, Producer's Accuracy (PA) was employed to represent the completeness of reference data (where high PA corresponds to low omission error). At the same time, User's Accuracy (UA) measured the reliability of map classes (where high UA corresponds to low commission error) (Olofsson et al., 2014). To address sample imbalance and harmonize the trade-off between PA and UA while avoiding the common misinterpretations associated with the Kappa coefficient in multi-class classification, this study prioritizes reporting results based on these class-specific metrics, following the latest recommendations in modern remote sensing literature (Foody, 2020). This approach ensures transparency in error assessment and enables reliable comparisons across different research periods and model configurations. To assess the reliability of the LULC classification, two rigorous validation indices were utilized: Overall Accuracy (OA) and the Kappa (Talukdar et al., 2020).

To quantify classification quality, three primary metrics were employed: Overall Accuracy (OA), Kappa Coefficient (K) (Talukdar et al., 2020).

Overall Accuracy (OA): OA is the percentage of correctly classified samples:

$$OA = \frac{TP+TN}{TP+TN+FP+FN} \times 100 \quad (6)$$

Where: TP (True Positive) = correct affirmative, TN (True Negative) = correct negative, FP (False Positive) = incorrect affirmative, FN (False Negative) = incorrect negative.

Kappa Coefficient (K), also known as Cohen's Kappa, measures the agreement between the classification and reference data after accounting for chance:

$$K = \frac{P_o - P_e}{1 - P_e} \quad (7)$$

Where: Po and Pe are the observed agreement proportion and the expected chance agreement, respectively.

Producer's Accuracy (PA): The probability that the classifier correctly identifies a reference pixel. It is a measure of omission error.

$$PA_i = \frac{n_{ii}}{n_{+i}} \quad (8)$$

Where: n_{ii} is the number of correctly classified pixels in class i, and n_{+i} is the total number of reference pixels in that class (column total).

User's Accuracy (UA): UA measures the probability that a pixel classified on the map actually represents that category on the ground. It is a measure of commission error.

$$UA_i = \frac{n_{ii}}{n_{i+}} \quad (9)$$

Where: n_{ii} is the number of correctly classified pixels in class i, and n_{i+} is the total number of pixels classified into that class on the map (row total).

2.3.6. Spatial analysis and urban expansion metrics

To quantify the spatial dynamics of Dien Bien Phu City, two primary metrics were employed: Urbanization Ratio (UR) and Urban Growth Rate (UGR). The UR represents the proportion of built-up area relative to total land area at a given time and serves as a key indicator of urban footprint density (M. Chen et al., 2016; United Nations, 2018). The UGR measures the intensity of urban expansion over a given period, using an exponential growth model to provide a standardized annual rate for cross-period comparisons of urbanization speed (Li et al., 2019; Seto et al., 2011). These metrics ensure consistent evaluation of urbanization trends in alignment with international urban monitoring standards (Schneider & Woodcock, 2008).

3. Results and Discussions

3.1. Sensitivity of different machine learning methods

Selecting an appropriate classification algorithm is crucial to ensuring the reliability of land use and land cover (LULC) maps, especially in regions with complex terrain like Dien Bien Phu City. In this study, the performance of two prominent machine learning classifiers, Random Forest (RF) and Support Vector Machine (SVM), was evaluated across eight years (2018–2025). The comparative results, measured by Overall Accuracy (OA) and Kappa coefficient, are summarized in Table 3.

Table 3. Comparative performance of Random Forest (RF) and Support Vector Machine (SVM) classifiers for LULC mapping from 2018 to 2025

No	Date of acquisition	Random Forest (RF)		Support Vector Machine (SVM)	
		Overall Accuracy	Kappa	Overall Accuracy	Kappa
1	14/02/2025	0.987	0.982	0.952	0.935
2	05/02/2024	0.977	0.971	0.937	0.914
3	26/01/2023	0.982	0.976	0.935	0.913
4	26/01/2022	0.942	0.962	0.931	0.901
5	25/02/2021	0.955	0.971	0.941	0.930
6	17/01/2020	0.988	0.984	0.951	0.927
7	21/02/2019	0.962	0.972	0.958	0.942
8	11/02/2018	0.974	0.960	0.936	0.912

The empirical results consistently demonstrate that the Random Forest (RF) algorithm outperforms the Support Vector Machine (SVM) across all observed years. The OA for RF remained remarkably high, ranging from 0.942 to 0.988, with the highest accuracy achieved in 2020 (OA = 0.988, Kappa = 0.984). In contrast, while SVM showed robust performance, its OA fluctuated between 0.931 and 0.958, generally trailing RF by approximately 2% to 5%. The Kappa statistics further reinforce this trend, with RF maintaining values consistently above 0.960 (except for a slight dip in 2022), indicating an "almost perfect" agreement between the classification results and ground truth data.

The superior performance of the RF model is primarily due to its ensemble learning architecture, which excels in navigating the high-dimensional feature space. By synergizing Sentinel-2 spectral bands (B2-B8 and B11-B12), essential remote sensing indices (NDVI, NDWI, NDBI), and DEM-derived topographic data, the model effectively enhances the separability of spectrally ambiguous classes, leading to more robust classification results. Specifically, RF's ability to mitigate overfitting and manage nonlinear relationships between spectral signatures and complex urban features (such as the mixture of built-up areas and bare soil) provided more stable results than SVM.

Although SVM performed well in 2019 (OA = 0.958), its sensitivity to hyperparameter tuning and the kernel choice made it slightly less consistent across different atmospheric conditions and seasonal variations inherent in the multi-temporal dataset. Consequently, the RF classifier was selected as the primary engine for generating the final LULC maps used in the urban development management analysis.

3.2. Relative importance of spectral bands, indices, and topographic data in the Random Forest classification for Dien Bien Phu City

The analysis of feature importance indicates that integrating multi-source data is pivotal for optimizing classification accuracy in Dien Bien Phu City. Notably, elevation emerges as the most influential variable, accounting for 12.5% of the total contribution. This underscores the critical role of topographic data in discriminating land cover classes within the region's complex basin-and-mountain terrain, where altitude often serves as a decisive factor in land-use distribution. Furthermore, the spectral indices NDVI (8.3%) and NDBI (8.3%) play a decisive role in distinguishing between vegetative cover and built-up areas. The superior weighting of these indices compared to individual spectral bands validates the effectiveness of feature engineering in enhancing the machine learning model's discriminative power (Fig. 3).

Beyond the calculated indices, the original Sentinel-2 spectral bands continue to make a significant and balanced contribution. Among the reflective bands, Band 8 (NIR) shows the highest importance at 8.8%, followed by the Red-edge bands (B7: 7.3%, B6: 6.8%, and B5: 6.6%), which collectively contribute approximately 20.7%. These bands are essential for capturing subtle chlorophyll absorption features and vegetation structure. The Short-Wave Infrared bands (B11: 9.1% and B12: 8.8%) also provide critical information for moisture content and urban surface characterization. Additionally, the NDWI (7.7%) significantly aids in identifying the Nam Rom River system and localized water bodies. This synergistic combination of multi-spectral information, indices, and geomorphological data not only minimizes spectral confusion between barren soil and urban structures but also establishes a robust classification framework essential for integrated urban development and planning management.

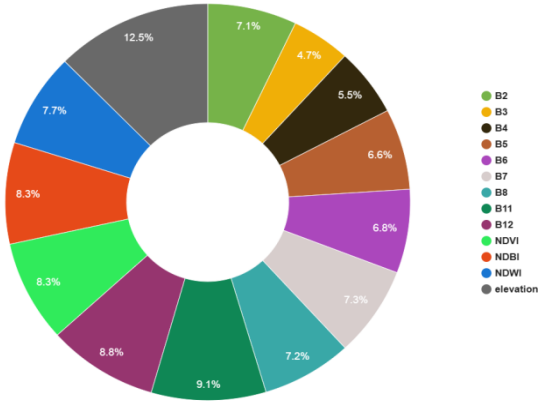

Figure 3. Contribution of different input sources

3.3. Maps of LULC classification

The period 2018–2025 (Fig. 4) marks a critical juncture in the landscape structural transformation of Dien Bien Phu City, illustrating the complex interplay between urban intensification and urban sprawl, which is a phenomenon typical of mountainous urban centers in Northern Vietnam. The proliferation of impervious surfaces, driven by urban expansion, has made urban land the primary driver of spatial reconfiguration.

This process is manifested through two synchronous trends: infill development within the Muong Thanh basin core and ribbon development along strategic transport corridors. A direct consequence of this shift is the substantial depletion of agricultural and ecological "matrices" that historically accommodated infrastructure demands. This

intensive conversion, concentrated in the transition zones between the historical core and the periphery, has fragmented traditional agricultural landscapes and exerted significant pressure on regional sustainability. Notably, while the forest massifs in Thanh Minh and Ta Leng remain dominant in overall extent, the emergence of localized edge degradation serves as a critical diagnostic signal. These subtle perforations in the green cover not only denote anthropogenic disturbances but also reflect the repercussions of infrastructure encroachment on forest ecological integrity, posing a formidable challenge in reconciling urban modernization objectives with long-term biodiversity conservation.

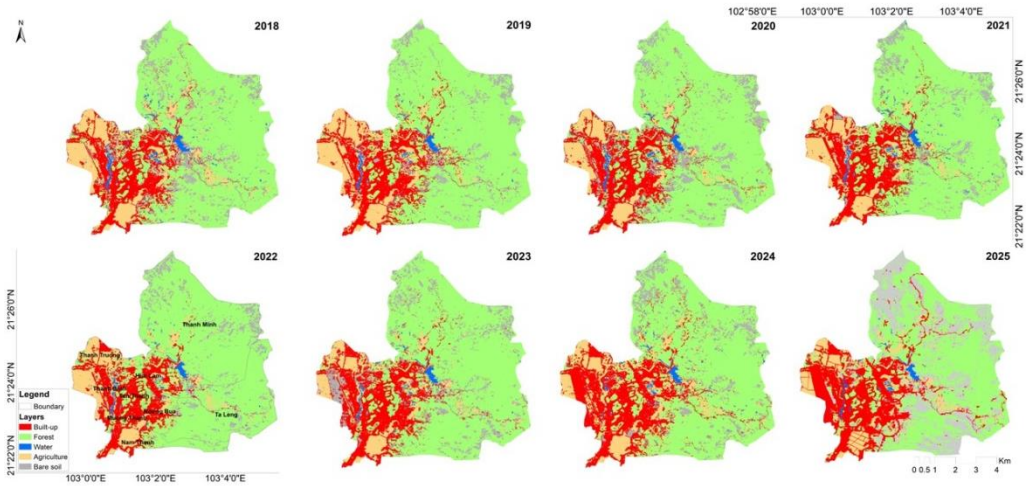

Figure 4. Land use/land cover maps of Dien Bien Phu in 2018 and 2025

3.4. Accuracy Assessment

The reliability of the LULC classification for Dien Bien Phu City was rigorously validated using a comprehensive multi-temporal confusion matrix for the period 2018–2025. Validation samples were strategically collected through the visual interpretation of high-resolution imagery from Google Earth and PlanetScope, with total sample sizes ranging from 800 (in 2019) to 1,433 (in 2023) points per year (Table 4). The assessment focused on four key performance indicators: User's Accuracy (UA), Producer's Accuracy (PA), Overall Accuracy (OA), and the Kappa coefficient.

The classification results demonstrate exceptional and stable performance over the 2018–2025 period, with Overall Accuracy (OA) ranging from 0.942 to 0.988 and Kappa coefficients (0.960–0.984) consistently indicating a high level of agreement with reference data. This robust precision is driven by the integrated use of multi-source remote sensing and the Random Forest algorithm, which effectively resolved spectral complexities across all land cover categories. Notably, the model achieved high discriminative power for Built-up (UA up to 0.994) and Forest (PA up to 0.995) classes by leveraging Red-edge bands and NDVI, while successfully distinguishing Water bodies and Agriculture from Barren Soil in mountainous terrains with precision metrics frequently exceeding 0.970. The inclusion of NDBI and DEM-derived topographic data was pivotal in mitigating spectral confusion, providing a reliable scientific foundation for long-term urban development analysis.

In summary, the high OA (surpassing 94% in all years) and robust Kappa statistics

(above 0.96) validate the LULC datasets as a highly reliable scientific foundation. These results ensure that subsequent analyses of urban expansion and planning management in Dien Bien Phu City are based on high-fidelity geographic information.

Table 4. Confusion Matrix of classified land use/land cover objects

LULC	*BU*	*F*	*W*	*A*	*BS*	Total	PA	UA	OA
2018									
BU	132	0	0	0	0	132	0.956	0.971	
F	0	411	0	0	4	415	0.976	0.980	
W	0	0	126	0	0	126	0.975	0.968	
A	3	0	1	144	0	148	0.915	0.973	
BS	3	0	0	0	158	161	0.975	0.981	
Total	138	411	127	144	162	**982**			
Kappa	**0.960**								**0.974**
2019									
BU	133	0	0	0	1	134	0.981	0.942	
F	0	347	1	0	2	350	0.977	0.951	
W	0	0	132	0	0	132	0.985	0.971	
A	0	1	1	108	0	110	0.956	0.962	
BS	0	0	0	0	74	74	0.961	0.985	
Total	133	348	134	108	77	**800**			
Kappa	**0.972**								**0.962**
2020									
BU	122	0	0	0	2	124	0.938	0.984	
F	2	393	1	1	1	398	0.995	0.987	
W	0	0	168	0	0	168	0.994	0.985	
A	5	0	0	294	0	299	0.997	0.983	
BS	1	0	0	0	106	107	0.972	0.991	
Total	130	393	169	295	109	**1096**			
Kappa	**0.984**								**0.988**
2021									
BU	146	0	0	0	0	146	0.973	0.926	
F	1	553	0	2	2	559	0.985	0.941	
W	0	0	123	1	0	124	0.962	0.971	
A	0	0	0	129	2	131	0.977	0.935	
BS	3	0	0	0	88	91	0.956	0.967	
Total	150	553	123	132	92	**1051**			
Kappa	**0.971**								**0.955**
2022									
BU	255	0	0	1	3	259	0.978	0.982	
F	0	587	0	0	0	587	0.980	0.952	
W	0	0	119	0	0	119	0.962	0.906	
A	0	0	0	193	0	193	0.925	0.928	
BS	5	0	0	0	80	85	0.964	0.941	
Total	260	587	119	194	83	**1243**			
Kappa	**0.962**								**0.942**
2023									
BU	300	0	0	1	6	307	0.958	0.977	
F	0	498	0	1	1	500	0.905	0.986	
W	0	0	114	1	0	115	0.961	0.951	
A	0	0	1	120	0	121	0.968	0.976	
BS	13	0	0	1	376	390	0.982	0.964	
Total	313	498	115	124	383	**1433**			
Kappa	**0.976**								**0.982**

LULC	*BU*	*F*	*W*	*A*	*BS*	Total	PA	UA	OA
2024									
BU	260	0	3	0	2	265	0.985	0.981	**0.977**
F	1	447	1	3	1	453	0.982	0.977	
W	0	0	104	1	0	105	0.945	0.980	
A	0	0	2	136	0	138	0.971	0.985	
BS	2	0	0	0	98	100	0.970	0.962	
Total	263	447	110	140	101	**1061**			
Kappa		**0.971**							
2025									
BU	174	0	0	0	0	174	0.994	0.994	
F	0	453	3	4	1	461	0.993	0.984	
W	0	3	128	1	0	132	0.970	0.970	
A	0	0	1	177	0	178	0.973	0.994	**0.987**
BS	1	0	0	0	118	119	0.992	0.992	
Total	175	456	132	182	119	**1064**			
Kappa		**0.982**							

3.5. Dynamics and transitions of land-cover types

Quantitative analysis of Fig. 5 and Table 5 reveals a profound structural transformation in Dien Bien Phu's landscape between 2018 and 2025. The built-up (BU) area expanded significantly, increasing from 8.8% to 12.4% of the total area. The transition matrix (Table 5) confirms that this urban growth primarily encroached upon agricultural land (231.10 ha) and forest areas (152.68 ha) during the 2021–2025 period. Notably, the expansion of BU often follows a multi-stage process where natural land is first cleared into Barren Soil (BS) before being developed into infrastructure. This is evidenced by the 83.05 ha of BS in 2021 that was converted into BU by 2025, alongside the high retention rate of existing BU (84.73%).

The most dramatic shift occurred in the Barren Soil (BS) and Forest (F) classes. BS coverage surged from 5.5% in 2018 to 14.1% in 2025, reflecting an intensification of surface disturbance. The transition matrix reveals that a staggering 1,124.83 ha of Forest land was converted to Barren Soil between 2021 and 2025 alone. This massive conversion, coupled with a decline in forest cover from 35.1% to 26.7%, suggests extensive land clearance for strategic infrastructure development and potentially for plantation harvesting cycles. Meanwhile, Agricultural (A) land decreased from 8.3% to 5.0%, as fertile valley lands were gradually absorbed by urban sprawl, particularly along the southwestern expansion corridors.

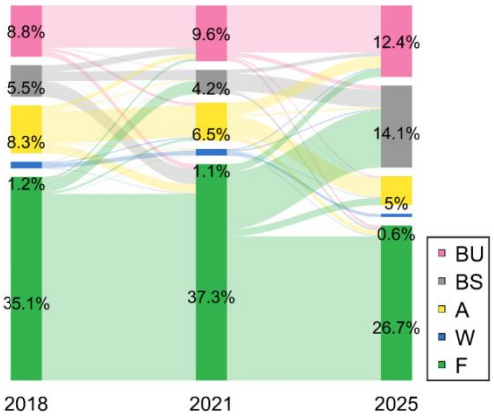

Figure 5. Proportion changes in LULC classes within the study area from 2018 to 2025

The observed transition patterns underscore an infrastructure-driven model of urbanization, with increasing pressure on peri-urban and forested landscapes. The substantial proportion of BS (14.1%) in 2025 serves as a transitional indicator, signaling significant potential for continued urban growth in the near future as these cleared sites are developed. However, the rapid conversion of

forests and agricultural land raises critical concerns about ecological stability. In the mountainous basin of Dien Bien Phu, such large-scale land-cover conversion may amplify environmental risks, necessitating an integrated management approach that aligns urban development with the sustainable preservation of natural resources.

Table 5. Land use/land cover transition matrix from 2018 to 2025

	Land-cover types	BU	F	W	A	BS	Total
		2018 (ha)					
2021 (ha)	**BU**	830.82	43.51	3.43	89.45	128.56	**1095.77**
	F	99.31	3665.06	10.86	183.98	298.43	**4257.64**
	W	4.81	7.70	87.62	20.11	5.54	**125.78**
	A	56.19	39.01	24.33	619.68	5.94	**745.16**
	BS	15.05	248.01	5.29	28.25	187.33	**483.93**
	Total	**1006.17**	**4003.29**	**131.53**	**941.47**	**625.81**	**6708.26**
		2021 (ha)					
2025 (ha)	**BU**	928.41	152.68	21.93	231.10	75.26	**1409.38**
	F	53.66	2834.05	12.99	93.22	52.59	**3046.50**
	W	0.98	1.51	55.15	8.98	0.45	**67.07**
	A	29.59	144.36	11.01	378.53	7.32	**570.81**
	BS	83.05	1124.83	24.69	33.26	348.31	**1614.14**
	Total	**1095.71**	**4257.42**	**125.77**	**745.10**	**483.92**	**6707.92**
		2018 (%)					
2021 (%)	**BU**	82.57	1.09	2.61	9.50	20.54	**82.57**
	F	9.87	91.55	8.26	19.54	47.69	**9.87**
	W	0.48	0.19	66.62	2.14	0.89	**0.48**
	A	5.58	0.97	18.50	65.82	0.95	**5.58**
	BS	1.50	6.20	4.02	3.00	29.93	**1.50**
	Total	**100**	**100**	**100**	**100**	**100**	**100**
		2021 (%)					
2025 (%)	**BU**	84.73	3.59	17.44	31.02	15.55	**84.73**
	F	4.90	66.57	10.33	12.51	10.87	**4.90**
	W	0.09	0.04	43.85	1.21	0.09	**0.09**
	A	2.70	3.39	8.75	50.80	1.51	**2.70**
	BS	7.58	26.42	19.63	4.46	71.98	**7.58**
	Total	**100**	**100**	**100**	**100**	**100**	**100**

The spatial dynamics of urban expansion in Dien Bien Phu City over the 2018–2025 period are characterized by a highly concentrated core and strategic outward sprawling, as illustrated by the Urbanization Rate and Urban Growth Rate maps (Fig. 6). The urbanization ratio shows a clear monocentric pattern, with the highest density (80–100%, depicted in purple and dark red) concentrated in the central valley. This core represents the city's historical and administrative heart, where built-up infrastructure is nearly saturated. The green-to-yellow gradient (0–40%) radiating from the center toward the periphery illustrates the transitional zones between rural and urban land. Notably, the urban footprint aligns closely with the north-south axis of the Nam Rom River valley, constrained by surrounding steep topography, which limits dense development to the flatter basin areas.

The urban growth rate (ha/year) provides a more dynamic perspective on the city's recent development. While the central core remains densely built, the most intense growth (0.6–0.8 ha/year, shown in dark brown) is observed at the western and northwestern edges of the existing urban center. This spatial trend suggests a deliberate westward expansion policy, likely driven by new infrastructure

projects and the relocation of residential clusters. Small, fragmented patches of growth (0.2–0.4 ha/year) are also visible along major transport arteries extending toward the outskirts. This pattern of "infill" and "edge-expansion" underscores a transition from a compact historical town to a more modern, sprawling urban entity, reflecting the effective implementation of the local urban planning maps.

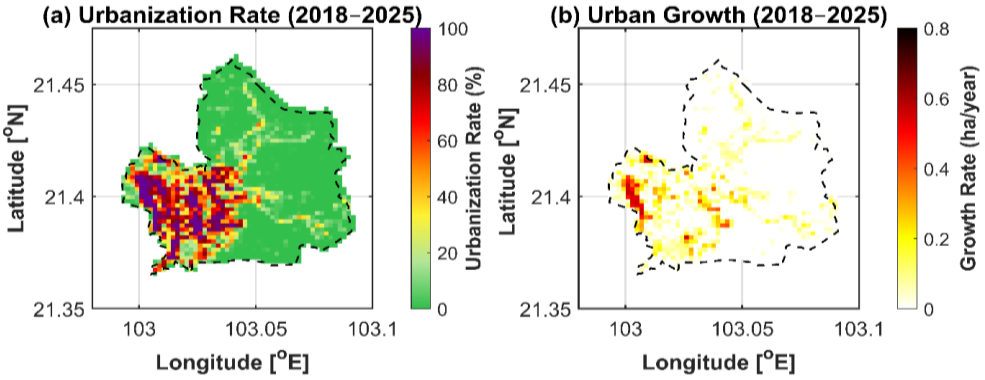

Figure 6. The distribution of the urbanization ratio and Urban growth rate in Dien Bien Phu

The synergy between high urbanization ratios in the center and high growth rates at the urban fringes highlights the dual challenge facing Dien Bien Phu's management: the need for urban renewal in the saturated core and the provision of sustainable infrastructure in the rapidly developing outskirts. These spatial insights provide a critical foundation for local authorities to balance urban growth with environmental preservation in a mountainous basin environment.

3.6. Urban development management

The 2025 land use/land cover analysis results, when cross-referenced with the Dien Bien Phu City Master Plan towards 2045, offer strategic insights into urban governance within a unique basin topography. With an OA of 98.7% and a K of 0.982 for the 2025 dataset, the remote sensing evidence demonstrates high reliability in monitoring planning implementation. These findings reflect a fundamental transition from a monocentric growth model to a polycentric structure, aligning seamlessly with the locality's long-term developmental vision.

The expansion of built-up areas as of 2025 exhibits a clear diffusion pattern, radiating from the historical core toward the East and South, particularly in the Noong Bua, Nam Thanh, and Ta Leng sectors. Overlay analysis (Fig. 7) reveals that a substantial portion of current agricultural and bare lands is situated within zones designated for future infrastructure development. Furthermore, the 2045 planning targets indicate a robust shift toward new growth poles in Noong Bua, Him Lam, and Thanh Minh, with projected occupancy rates increasing by 1.5 to 2 times those in 2025. As of 2025, the 24.1% share of bare soil serves as a potential land reserve for realizing these functional subdivisions.

In summary, the synergy between high-precision satellite observations and the 2045 Strategic Vision establishes a transparent framework for urban management. Maintaining high Producer's and User's Accuracy metrics, mostly exceeding 0.94, for built-up and agricultural classes provides a robust empirical foundation for enforcing planning boundaries. In the forthcoming phase, urban management in Dien Bien Phu should prioritize the realization of polycentric functional zones while closely

monitoring forest depletion at peri-urban fringes, such as Ta Leng and Thanh Minh, to preserve the distinctive landscape identity of the Dien Bien basin.

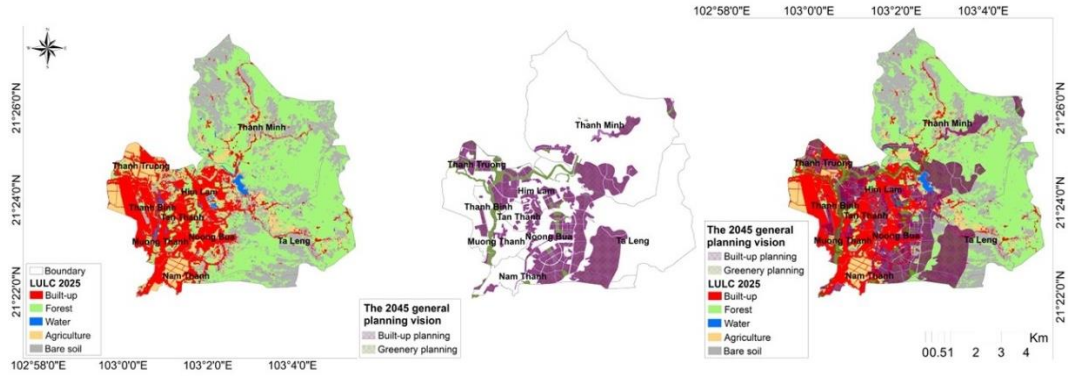

Figure 7. Integration of LULC 2025 derived from Sentinel-2 and the 2045 General Planning Vision for Dien Bien Phu City: From current state monitoring to strategic urban management

The results of this study provide a practical monitoring framework for urban development management in Dien Bien Phu City. First, the identification of a substantial increase in bare land (24.1%) highlights the need for stricter oversight of construction timelines to prevent prolonged land underutilization and soil erosion. Second, the spatial transition toward a polycentric model requires adjustments in infrastructure investment planning along the southern and western corridors. Finally, by benchmarking LULC changes against the 2045 Master Plan, this research provides an 'early warning' signal for potential conflict zones where urban expansion may threaten forest protection boundaries, enabling more proactive and climate-resilient spatial planning.

Table 6. Comparative analysis of the current built-up area (2025) and urban planning targets (2045) across administrative wards in Dien Bien Phu City

Name of the ward	Built-up area in 2025 (ha)	Built-up planning area in 2045 (ha)	Built-up area completed under planning (ha)	Urban plan implementation rate (%)
Him Lam	285.83	176.23	63.44	36.00
Muong Thanh	136.95	12.55	11.92	95.02
Nam Thanh	128.58	147.19	13.90	9.45
Noong Bua	178.60	101.89	34.65	34.01
Tan Thanh	79.28	0	0	-
Thanh Binh	70.72	1.93	1.18	61.40
Thanh Truong	320.24	124.40	33.07	26.59
Ta Leng	64.13	357.70	13.75	3.84
Thanh Minh	73.44	279.48	7.71	2.76

4. Discussions

4.1. Spatial Dynamics of Urbanization

The findings indicate that Dien Bien Phu City is undergoing a profound structural transformation. The annual urban expansion rate is significantly higher than that of typical delta cities, reflecting a broader trend of rapid modernization among regional administrative centers in mountainous Southeast Asia. However, unlike the concentric growth patterns often found in flat regions (Seto et al., 2012), urban development in Dien Bien Phu is strictly governed by its basin topography. This study confirms the theories proposed by Yang et al. (2021) and Zhang et al. (2024) regarding

the decisive role of terrain in shaping the spatial morphology of mountainous cities. Expansion is forced to follow valley floors and major transport corridors, primarily along the North-South axis of the Nam Rom River (Yang & Huang, 2021; Zhang & Han, 2024). Notably, the high proportion of Barren Soil (14.1% in 2025), a significant increase from 5.5% in 2018, acts as a precursor to future urban density. This transitional land cover suggests that the city is in a state of "active preparation," where large-scale site clearances for infrastructure projects are set to transition into permanent built-up structures in the coming phase of the 2045 General Planning.

4.2. Conflict between Urban Expansion and Ecological Security

The rapid depletion of forest cover (from 35.1% to 26.7%) and the encroachment of urban expansion into mountain foothills, particularly in Thanh Minh and Ta Leng, pose critical threats to ecological security. The conversion of forest land directly into Barren Soil (1,124.83 ha between 2021 and 2025) not only disrupts vital green corridors but also exacerbates the risks of debris flows and landslides. While the 2045 General Planning proposes expansions into higher elevation zones, terrain slope remains a non-negotiable constraint. As established by Yang et al. (2021) and Zhang et al. (2024), the most suitable slope for sustainable construction is 0–6° (Yang & Huang, 2021; Zhang & Han, 2024). Our analysis reveals that recent expansion is pushing these limits, increasing geological instability. Consequently, urban managers must prioritize "Nature-based Solutions" (NbS) and reconsider construction density in high-slope sectors. Strengthening protection of forest boundaries and integrating green infrastructure are essential to enhancing climate resilience in this vulnerable basin.

4.3. Reliability of the Analytical Framework

The reliability of this monitoring process is ensured by an analytical framework that synthesizes multi-temporal Sentinel-2 imagery, a SRTM DEM, and the Random Forest algorithm. The classification performance achieved (OA up to 98.8%, Kappa 0.984) aligns with and exceeds recent research by Thanh Noi et al. (2020) in Northern Vietnam. The integration of Red-edge bands and topographic indices effectively mitigated spectral confusion between built-up areas and barren soil a common challenge in fragmented mountainous terrains. This empirical evidence provides a robust scientific foundation for adjusting planning boundaries and ensuring that the 2045 Vision is based on high-fidelity, data-driven insights.

5. Conclusions

This study provides a comprehensive assessment of urbanization dynamics in Dien Bien Phu City from 2018 to 2025 by integrating multi-source remote sensing data and machine learning. The findings reveal a significant structural shift: Built-up areas expanded by 41% (from 8.8% to 12.4%), primarily driven by the conversion of agricultural and forest lands through an intermediate stage of barren soil. The spatial morphology shows a dual trend: a consolidating high-intensity core in the central basin and a strategic expansion toward the western and southern corridors following a grid pattern. However, the substantial decline in forest cover within a short seven-year period raises urgent sustainability concerns, as it increases ecological vulnerability and exposure to natural hazards in peri-urban mountainous zones.

The integrated framework (Sentinel-2, DEM, and RF algorithm) achieved exceptional accuracy, meeting the rigorous standards required for advanced urban planning management. From a governance perspective, the newly developed velocity and intensity maps provide critical empirical evidence for auditing the 2045 General

Planning Vision. We suggest that local authorities prioritize green infrastructure strategies, such as strictly enforcing forest protection boundaries and utilizing existing barren lands for ecological functions, to mitigate the Urban Heat Island (UHI) effect and landslide risks.

Future research should explore integrating Synthetic Aperture Radar (SAR) from Sentinel-1 to overcome cloud-cover limitations and provide deeper insights into structural building density. Additionally, applying advanced deep learning approaches, such as Convolutional Neural Networks (CNNs) or Vision Transformers, could further improve classification performance in highly complex terrains. Incorporating long-term climate variables will be essential to evaluate the interaction between rapid urban sprawl and microclimate resilience in mountainous basin-style cities.

Acknowledgments

This research was funded by the Ministry of Science and Technology (MOST), Vietnam, through the project "Research and application of machine learning in multi-source satellite data processing for air pollution mapping to assess its impact on public health and analyze its correlation with urbanization and emission sources" (grant No. NĐT/US/24/04).

The authors would like to thank Planet Labs for providing free PS satellite observations, which have been utilized in this work through the Planet's Education and Research Program.

References

Acharki S., 2022. PlanetScope contributions compared to Sentinel-2, and Landsat-8 for LULC mapping. Remote Sensing Applications: Society and Environment, 27, 100774. https://doi.org/10.1016/j.rsase.2022.100774.

Azizi P., Soltani A., Bagheri F., Sharifi S., Mikaeili M., 2022. An Integrated Modelling Approach to Urban Growth and Land Use/Cover Change. Land, 11(10), 1715. https://doi.org/10.3390/land11101715.

Belcore E., Piras M., Wozniak E., Email I., 2020. Specific alpine environment land cover classification methodology : Google Earth Engine processing for Sentinel-2 data. The International Archives of the Photogrammetry, Remote Sensing and Spatial Information Sciences, XLIII, 663–670. https://doi.org/10.5194/isprs-archives-XLIII-B3-2020-663-2020.

Belgiu M., Drăguţ L., 2016. Random forest in remote sensing: A review of applications and future directions. ISPRS Journal of Photogrammetry and Remote Sensing, 114, 24–31. https://doi.org/10.1016/j.isprsjprs.2016.01.011.

Breiman L., 2001. Random Forests. Machine Learning, 45(1), 5–32. https://doi.org/10.1023/A:1010933404324.

Chen M., Liu W., Lu D., 2016. Challenges and the way forward in China's new-type urbanization. Land Use Policy, 55, 334–339. https://doi.org/10.1016/j.landusepol.2015.07.025.

Chen X.-L., Zhao H.-M., Li P.-X., Yin Z.-Y., 2006. Remote sensing image-based analysis of the relationship between urban heat island and land use/cover changes. Remote Sensing of Environment, 104(2), 133–146. https://doi.org/10.1016/j.rse.2005.11.016.

Delalay M., Ziegler A.D., Passy P., Delalay M., Tiwari V., Ziegler A.D., Gopal V., Passy P., 2019. Classification using Sentinel-2 data and machine-learning algorithms : operational method and its implementation for a mountainous area of Nepal. Journal of Applied Remote Sensing, 13(1), 014530. https://doi.org/10.1117/1.JRS.13.014530.

Dien Bien Province Department of Natural Resources and Environment, 2024. Dien Bien Province Environmental Report, 1–15.

Dien Bien Provincial Statistics Department, 2024. DienBien statistical yearbook 2023. https://thongkedienbien.nso.gov.vn/.

Drusch M., Del Bello U., Carlier S., Colin O., Fernandez V., Gascon F., Hoersch B., Isola C., Laberinti P., Martimort P., Meygret A., Spoto F., Sy O., Marchese F., Bargellini P., 2012. Sentinel-2: ESA's Optical High-Resolution Mission for GMES Operational Services. Remote Sensing of Environment, 120, 25–36. https://doi.org/10.1016/j.rse.2011.11.026.

Foody G.M., 2020. Explaining the unsuitability of the kappa coefficient in the assessment and comparison

of the accuracy of thematic maps obtained by image classification. Remote Sensing of Environment, 239, 111630. https://doi.org/https://doi.org/10.1016/j.rse.2019.111630.

Herold M., Goldstein N.C., Clarke K.C., 2003. The spatiotemporal form of urban growth: measurement, analysis and modeling. Remote Sensing of Environment, 86(3), 286–302. https://doi.org/10.1016/S0034-4257(03)00075-0.

Houborg R., McCabe M., 2016. High-Resolution NDVI from Planet's Constellation of Earth Observing Nano-Satellites: A New Data Source for Precision Agriculture. Remote Sensing, 8(9), 768. https://doi.org/10.3390/rs8090768.

Hung N.M., Anh T.V., Duy T.D., Mai S. Le, Cong G.N., Le H., Thu T., 2025. Urban Expansion Monitoring Using Sentinel-1 and Sentinel-2 Data Fusion on Google Earth Engine. International Conference on Earth, Mine and Environmental Sciences for Green, Sustainable, and Prosperous Development in the Era of a Nation's Rise (EME2025), 2, 180–189. https://doi.org/10.15625/vap.2025.0196.

Le-Tuan P., Vu Vinh B., Manh Pham V., Thi Lan Anh N., Huy Nguyen Q., Huu Duy N., Thanh Bui Q., 2025. Automated dense-layer architecture search on EfficientNet: A hybrid approach for scene-based land-cover classification. Vietnam Journal of Earth Sciences, 47(3), 396–410. https://doi.org/10.15625/2615-9783/23402.

Li M., van Vliet J., Ke X., Verburg P.H., 2019. Mapping settlement systems in China and their change trajectories between 1990 and 2010. Habitat International, 94, 102069. https://doi.org/10.1016/j.habitatint.2019.102069.

Ma L., Liu Y., Zhang X., Ye Y., Yin G., Johnson B.A., 2019. Deep learning in remote sensing applications: A meta-analysis and review. ISPRS Journal of Photogrammetry and Remote Sensing, 152, 166–177. https://doi.org/10.1016/j.isprsjprs.2019.04.015.

Manoli G., Fatichi S., Schläpfer M., Yu K., Crowther T.W., Meili N., Burlando P., Katul G.G., Bou-Zeid E., 2019. Magnitude of urban heat islands largely explained by climate and population. Nature, 573(7772), 55–60. https://doi.org/10.1038/s41586-019-1512-9

McFeeters S.K., 1996. The use of the Normalized Difference Water Index (NDWI) in the delineation of open water features. International Journal of Remote Sensing, 1425–1432. https://doi.org/10.1080/01431169608948714.

Ministry of Construction & People's Committee of Dien Bien Province, 2024. Dien Bien Province Planning for the period 2021–2030, with a vision to 2050 (Decision No. 109/QD-TTg dated January 27, 2024 of the Prime Minister). https://xaydungchinhsach.chinhphu.vn/quy-hoach-tinh-dien-bien-4-truc-dong-luc-3-vung-kinh-te-4-cuc-tang-truong-119240128193402484.htm.

Ngo Van L., Nguyen H., Dang Kinh B., Giang Tuan L., Dang Van B., Do Trung H., Nguyen Minh H., Dang Nguyen V., Dao Minh D., 2025. Advancing debris flow detection based on deep learning model and high-resolution images. Vietnam Journal of Earth Sciences, 47(2), 290–314. https://doi.org/10.15625/2615-9783/23027.

Nguyen H.D., Pham V.T., Nguyen Q.-H., Bui Q.-T, 2025. Soil salinity prediction using satellite-based variables and machine learning: Case study in Tra Vinh province, Mekong Delta, Vietnam. Vietnam Journal of Earth Sciences, 47(2), 201–219. https://doi.org/10.15625/2615-9783/22438.

Nguyen Thanh H., Ho Le T., Nguyen Van D., Hoa Thuy Q., Nguyen Kim A., Le Duc H., Pham Van D., Phan Trong T., Tran Van P., 2025. Forest cover change mapping based on Deep Neuron Network, GIS, and High-resolution Imagery. Vietnam Journal of Earth Sciences, 47(2), 157–181. https://doi.org/10.15625/2615-9783/22192.

Nguyen Thi Phuong N., Tran Ba D., Do Dieu L., 2022. Assessing the Potential of Community-Based Ecotourism Toward Sustainable Development: a Case Study in Tua Chua Karst Plateau - Dien Bien - Viet Nam. Geojournal of Tourism and Geosites, 44(4), 1300–1305. https://doi.org/10.30892/gtg.44414-946.

Nguyen Trinh Duc H., Nguyen Hao Q., Tri Nguyen Q., Tran Duc D., Vo Thi H., Nguyen Phuong L., Phuong Lan N., Nguyen Dang Huyen T., Sergey G., Le Van D., Dang Ngoc Thi G., Ha Nam T., 2025. Machine learning approaches for satellite-derived bathymetry in tropical coastal waters: A comparative study from Nha Trang marine protected area, Vietnam. Vietnam Journal of Earth Sciences. https://doi.org/10.15625/2615-9783/24020.

Olofsson P., Foody G.M., Herold M., Stehman S.V, Woodcock C.E., Wulder M.A., 2014. Good practices for estimating area and assessing accuracy of land

change. Remote Sensing of Environment, 148, 42–57. https://doi.org/10.1016/j.rse.2014.02.015.

Rouse W., Haas H., Deering W., 1974. Monitoring vegetation systems in the Great Plains with ERTS. NASA Special Publication.

Schneider A., Woodcock C.E., 2008. Compact, dispersed, fragmented, extensive? A comparison of urban growth in twenty-five global cities using remotely sensed data, pattern metrics and census information. Urban Studies, 45(3), 659–692. https://doi.org/10.1177/0042098007087340.

Seto K.C., Fragkias M., Güneralp B., Reilly M.K., 2011. A Meta-Analysis of Global Urban Land Expansion. PLoS ONE, 6(8), e23777. https://doi.org/10.1371/journal.pone.0023777.

Seto K.C., Güneralp B., Hutyra L.R., 2012. Global forecasts of urban expansion to 2030 and direct impacts on biodiversity and carbon pools. The Proceedings of the National Academy of Sciences (PNAS), 109(40) 16083–16088. https://doi.org/10.1073/pnas.1211658109.

Talukdar S., Singha P., Mahato S., Shahfahad Pal S., Liou Y.-A., Rahman A., 2020. Land-Use Land-Cover Classification by Machine Learning Classifiers for Satellite Observations A Review. Remote Sensing, 12(7), 1135. https://doi.org/10.3390/rs12071135.

Tamiminia H., Salehi B., Mahdianpari M., Quackenbush L., Adeli S., Brisco B., 2020. Google Earth Engine for geo-big data applications: A meta-analysis and systematic review. ISPRS Journal of Photogrammetry and Remote Sensing, 164, 152–170. https://doi.org/10.1016/j.isprsjprs.2020.04.001.

Thanh Noi P., Kuch V., Lehnert L.W., 2020. Land cover classification using google earth engine and random forest classifier-the role of image composition. Remote Sensing, 12(15), 2411. https://doi.org/10.3390/RS12152411.

United Nations, 2018. 68% of the world population projected to live in urban areas by 2050. Department of Economic and Social Affairs. https://www.un.org/uk/desa/68-world-population-projected-live-urban-areas-2050-says-un.

United Nations, 2022. World Population Prospects:The 2022 Revision. United Nations Department of Economic and Social Affairs, Population Division.

Weng Q., 2001. A remote sensing?GIS evaluation of urban expansion and its impact on surface temperature in the Zhujiang Delta, China. International Journal of Remote Sensing, 22(10), 1999–2014. https://doi.org/10.1080/713860788.

Weng Q., 2012. Remote sensing of impervious surfaces in the urban areas: Requirements, methods, and trends. Remote Sensing of Environment, 117, 34–49. https://doi.org/10.1016/j.rse.2011.02.030.

World Bank, 2014. Northern Mountains Urban Development Program - Vietnam. World Bank Project Appraisal Document, 2014(3), 1–9. https://documents.worldbank.org/en/publication/documents-reports/documentdetail/183141468134090716/vietnam-result-based-northern-mountains-urban-program-project.

Wulder M.A., Roy D.P., Radeloff V.C., Loveland T.R., Anderson M.C., Johnson D.M., Healey S., Zhu Z., Scambos T.A., Pahlevan N., Hansen M., Gorelick N., Crawford C.J., Masek J.G., Hermosilla T., White J.C., Belward A.S., Schaaf C., Woodcock C.E., J.L. Huntington, L. Lymburner, P. Hostert, F. Gao Lyapustin, J.F. Peke, P. Strobl, Cook B.D., 2022. Fifty years of Landsat science and impacts. Remote Sensing of Environment, 280, 113195. https://doi.org/10.1016/j.rse.2022.113195.

Xu H., 2006. Modification of normalised difference water index (NDWI) to enhance open water features in remotely sensed imagery. International Journal of Remote Sensing, *27*(14), 3025-3033. https://doi.org/10.1080/01431160600589179.

Yang J., Huang X., 2021. The 30 m annual land cover dataset and its dynamics in China from 1990 to 2019. Earth System Science Data, 13(8), 3907–3925. https://doi.org/10.5194/essd-13-3907-2021.

Yin H., Tan B., Frantz D., Radeloff V.C., 2022. International Journal of Applied Earth Observations and Geoinformation Integrated topographic corrections improve forest mapping using Landsat imagery. International Journal of Applied Earth Observation and Geoinformation, 108, 102716. https://doi.org/10.1016/j.jag.2022.102716.

Zha Y., Gao J., Ni S., 2003. Use of normalized difference built-up index in automatically mapping urban areas from TM imagery. International Journal of Remote Sensing, 24(3), 583–594. https://doi.org/10.1080/01431160304987.

Zhang X., Han H., 2024. Characteristics and factors influencing the expansion of urban construction land in China. Scientific Reports, 14(1), 16040. https://doi.org/10.1038/s41598-024-67015-8.

Zhou D., Xiao J., Bonafoni S., Berger C., Deilami K., Zhou Y., Frolking S., Yao R., Qiao Z., Sobrino J.A., 2019. Satellite remote sensing of surface urban heat islands: Progress, challenges, and perspectives. In Remote Sensing, 11(1), 48, MDPI AG. https://doi.org/10.3390/rs11010048.

APPENDIX

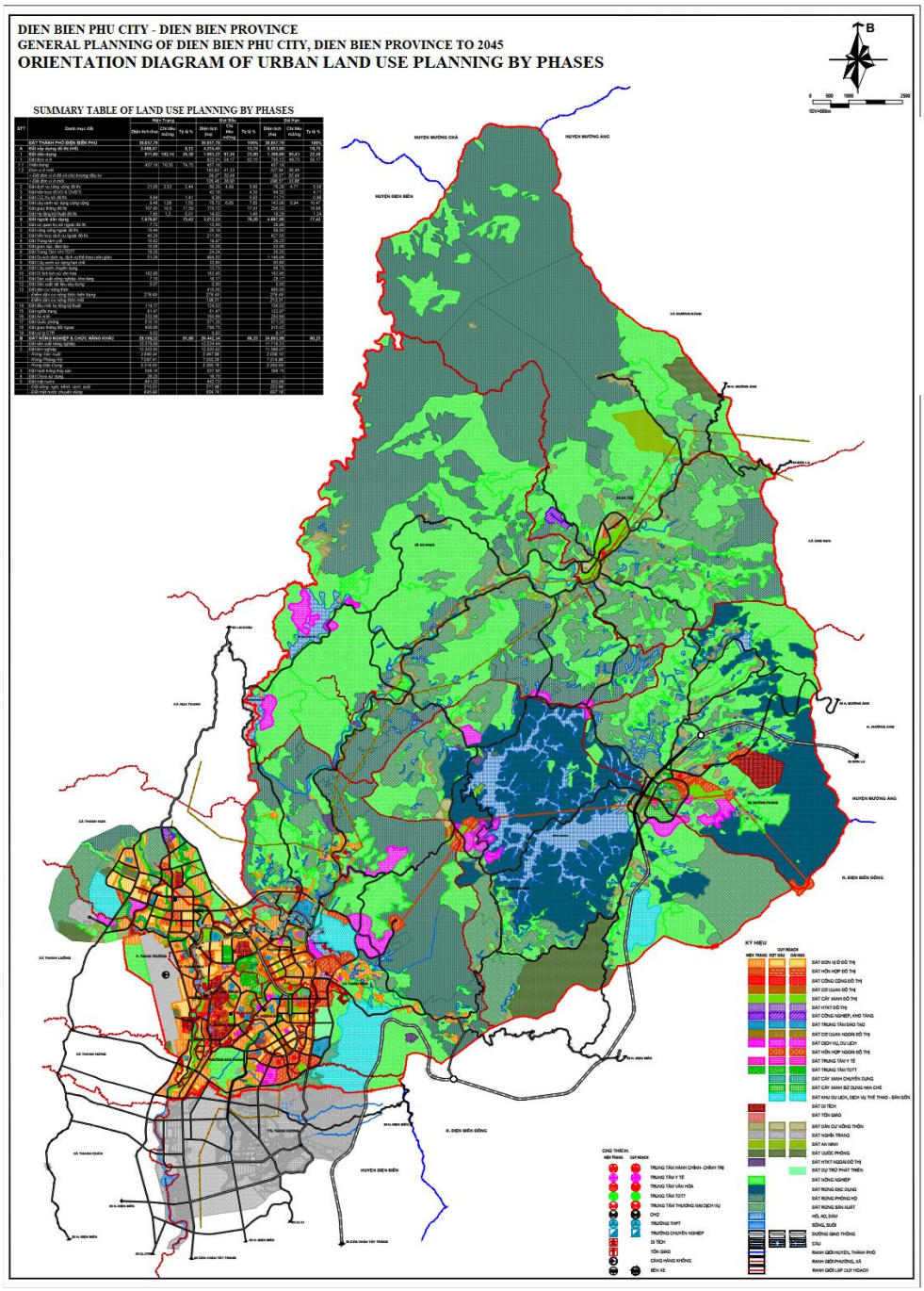

Source: Vietnam Institute for Urban and Rural Planning (VIUP)

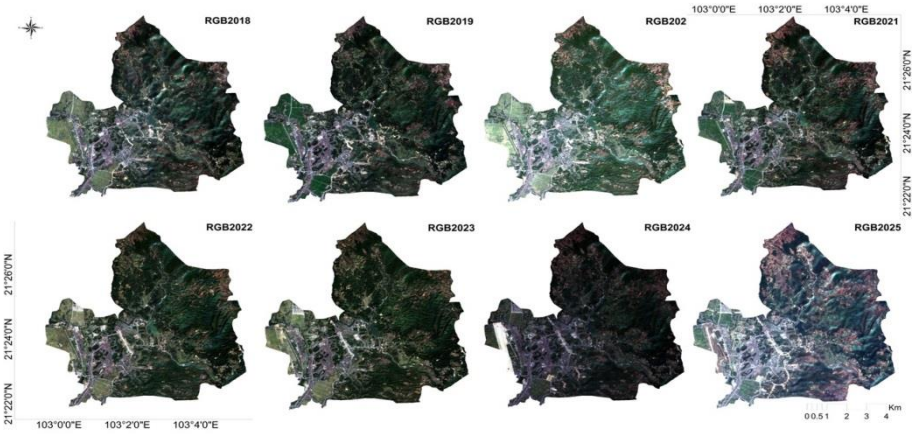

Figure 1A. RGB color composite of Sentinel-2 imagery, Dien Bien Phu City

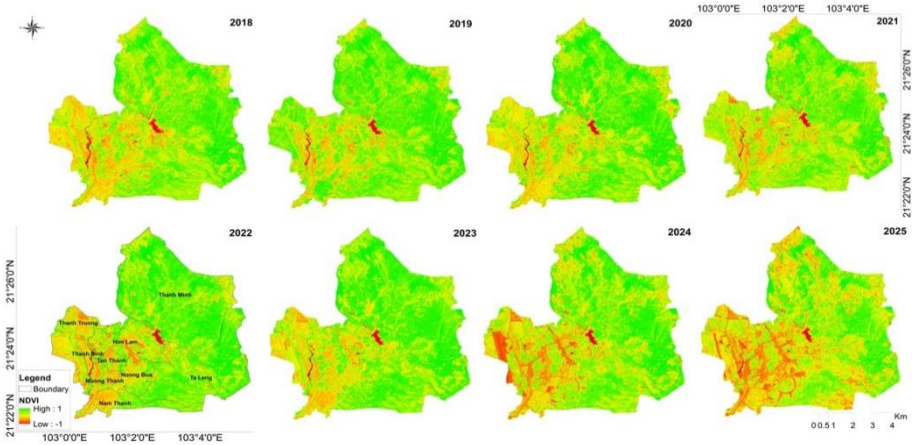

Figure 2A. NDVI derived from Sentinel-2 imagery, Dien Bien Phu City

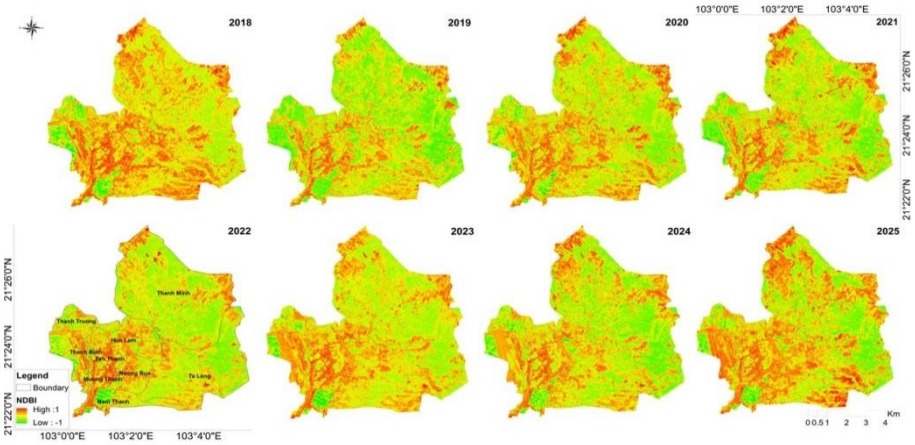

Figure 3A. NDBI derived from Sentinel-2 imagery, Dien Bien Phu City